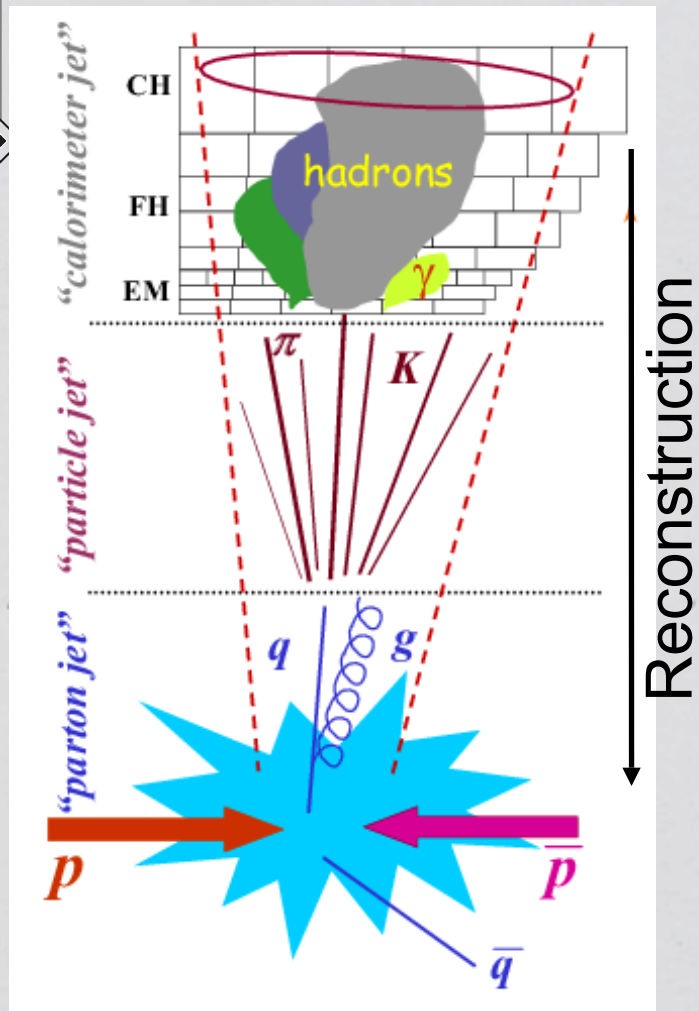

JET RECONSTRUCTION AND CALIBRATION

Additional material from: S. Menke, P. Francavilla and Z. Zenonos



Outlook

- * Introduction: jet calibration strategy in ATLAS
- * Additional material provided by ARTEMIS members:
 - * Z. Zenonos: “TileCal simulation studies: first results on validation of hadronic physics simulation”
 - * S. Menke: “Local hadron calibration”
 - * P. Francavilla: “Effect on inclusive jet cross section measurement of systematic uncertainties: first approach”



* Jet reconstruction consists in obtaining from the calorimeter hadronic signals the kinematics of the **particle jet** or of the **parton jet** depending on where we want to have Theory-Data comparison.

Parton jet, Particle jet, Calorimeter jets are obtained running the same jet clustering algorithm on:

- Partons
- stable particles after fragmentation
- calorimeter signals

Jet Reconstruction Algorithms

- * Jet clustering algorithms must be applicable at any level: calorimeter signals, particles, partons (jet components).

Various jet clustering algorithms have been implemented in ATLAS. Brief description of the two that are mostly used for physics analysis:



Iterative seeded cone algorithm



k_T algorithm

Once the jet components have been obtained the jet kinematics is calculated from the components applying the “**recombination scheme**”: the recombination scheme used in ATLAS is the 4-momentum sum of the jet components.

Jet clustering: iterative seeded cone algorithm

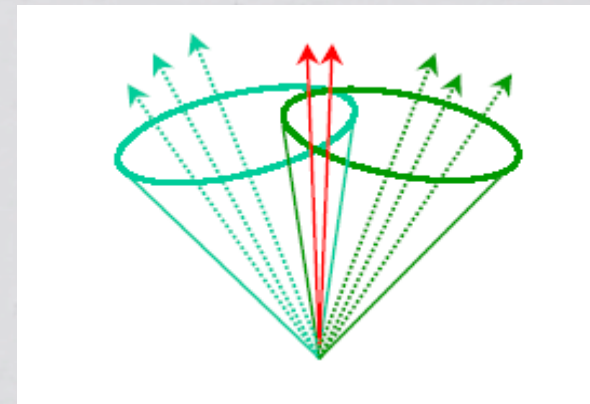
1. All jet components in (η, φ) having $E_T > E_{T,seed}$ are considered as **seeds** for the jets

2. For each seed (η^s, φ^s) all components lying at distance $< \Delta R$ are associated to the jet

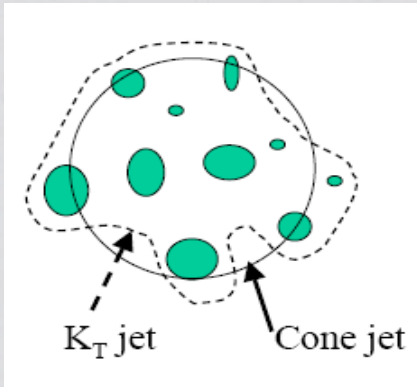
3. if the seed position (η^s, φ^s) coincide (< 0.05) with the jet centroide (η^c, φ^c) , the jet is considered stable otherwise $(\eta^s, \varphi^s) = (\eta^c, \varphi^c)$.

4. two jets sharing a percentual of energy energy $> \Delta S$ of the least energetic jets are combined, otherwise the shared components are associated to the closest jet.

	ΔR	$E_{T,seed}$	ΔS
ATLAS	0.4/0.7	1 GeV	50%
CMS	0.5	2 GeV	-
CDF	0.4/0.7	1 GeV	75%



Jet clustering algorithm : k_T



Jet components are clustered considering closeness in ΔR and transverse momentum (k_T). k_T jets do not have predefined geometrical shape.

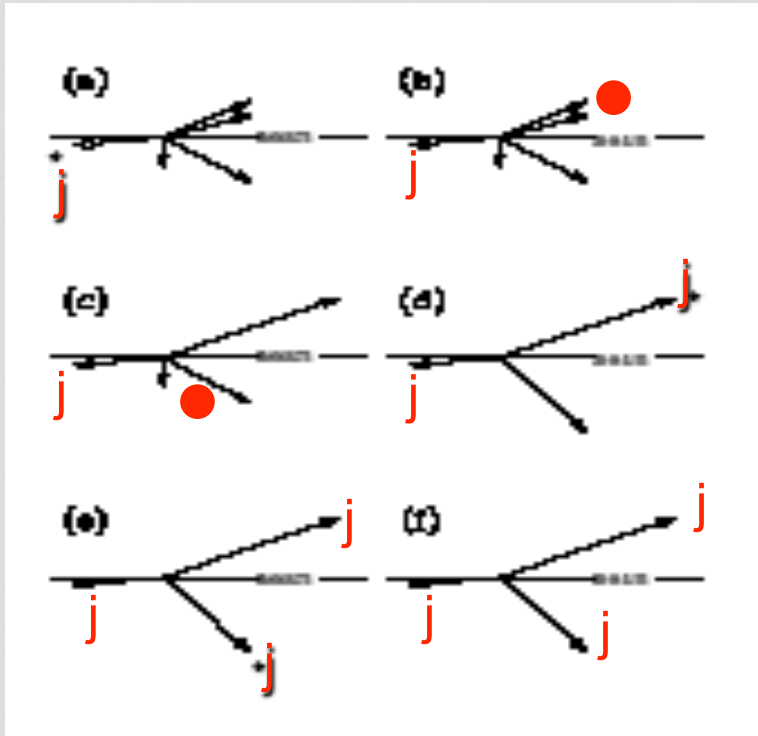
For each couple of components i, j

$$d_{ij} = p_{T,i}^2$$

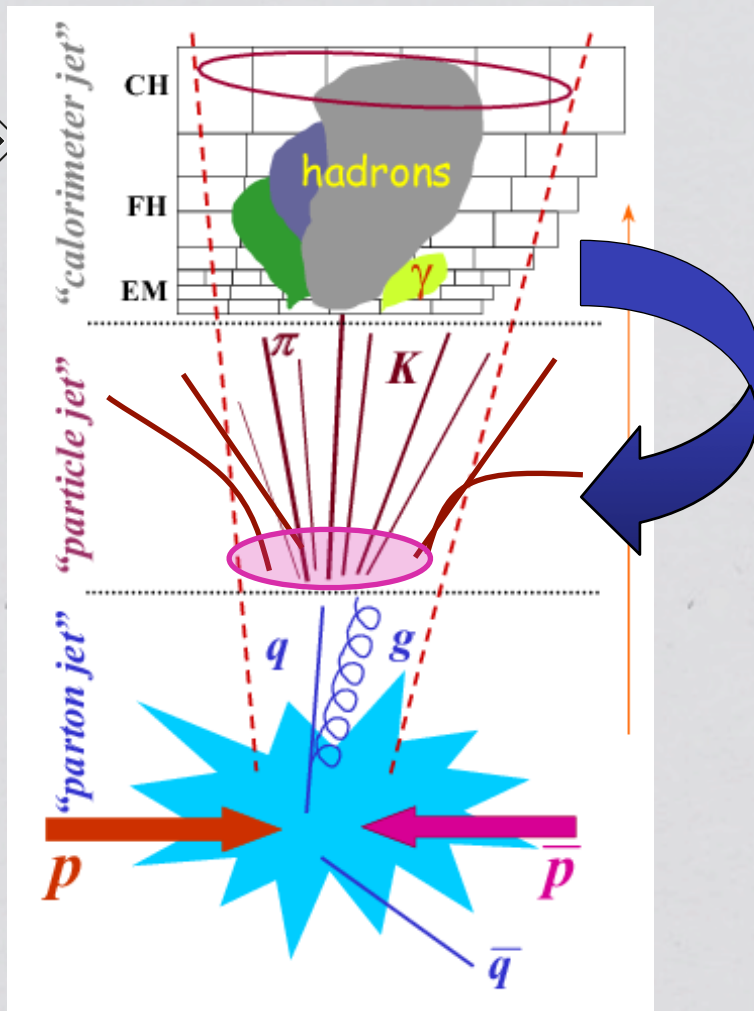
$$d_{ij} = \min(p_{T,i}^2, p_{T,j}^2) \frac{\Delta R_{ij}^2}{D^2} \quad \left. \begin{array}{l} \text{Collinear} \\ \text{(if } \Delta R \ll 1) \end{array} \right\}$$

Angular resolution

If $(d_{\min} = d_{ij}) \Rightarrow \text{jet}$
 else if $d_{\min} = d_{ij} \Rightarrow ij$ (4-vector sum)
 in a new d_{ij}



k_T algorithm is infrared and collinear safe



- * After jets have been reconstructed we need to correct energy measurement for detector effects:
 - * calorimeter non compensation (e/h)
 - * effect of cracks, dead material, losses in front of calorimeter, longitudinal leakage, magnetic field effect
- * Jet calibration methods discussed here:
 - * H1 -> I. Vivarelli
 - * Local Hadron Calib -> S. Menke
 - * Energy Flow -> M. Hodgkinson

MC validation studies: TileCal sampling fraction

Zenonos Zenonas

- * Many jet calibration schemes rely on how well Monte Carlo simulation (Geant4) predicts interacting particles with ATLAS calorimeters
- * Need to validate in detail Geant4 hadronic physics lists comparing results with test beam data
- * Just an example is shown here: evolution of TileCal sampling fraction with respect to different physics lists
- * Ongoing activities: Geant4 had. physics validation with CTB data (V. Kazanine, I. Vivarelli), Geant4/Fluka comparison with TileCal TB data (M.Cascella, I. Vivarelli, T. Del Prete, A.D.)

TileCal Sampling Fraction Studies

ATLAS Hadronic Calorimeter: a sampling calorimeter

- absorption of energy in high-density material (steel)
- scintillating tiles periodically sample the energy deposited
- infer the total energy of the original particle shower

TileCal Sampling Fraction: a constant parameter

- is used in the digitization step of MC simulation
- multiplies the energy deposits in the scintillators to get the calibrated energy released in TileCal

$$TSF = \frac{E_{vis}^{scint}}{E_{beam}}$$

energy deposited only in sensitive parts of cells -scintillators

energy deposited in TileCal cells

Tilerow 7

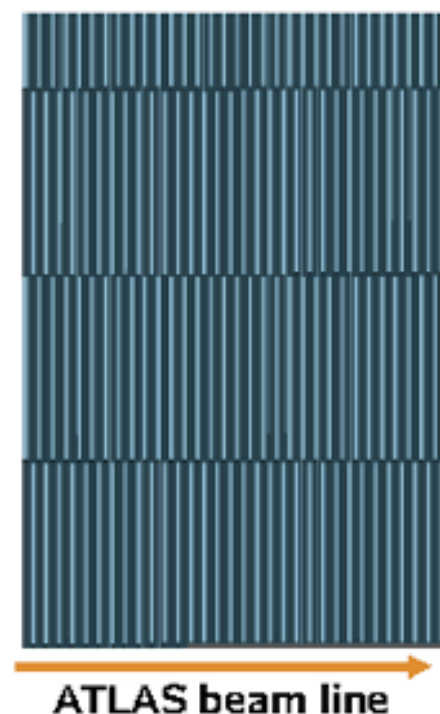
Tilerow 6

Tilerow 5

Physics List: MC particle physics data sets

- QGSP: Quark Gluon String-Model
- upgraded production cross-sections
- + theory driven model for final state

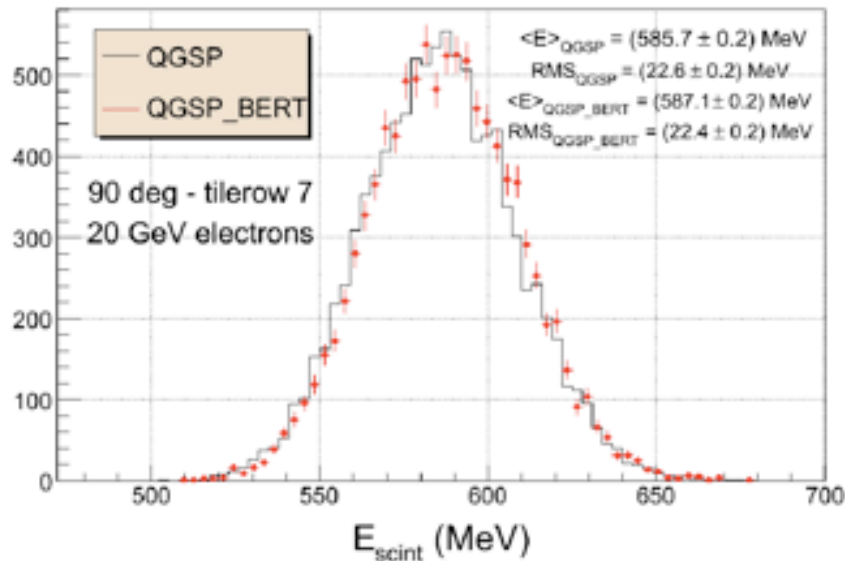
The periodical iron – scintillator TileCal structure



Details of electron simulation in ATLAS

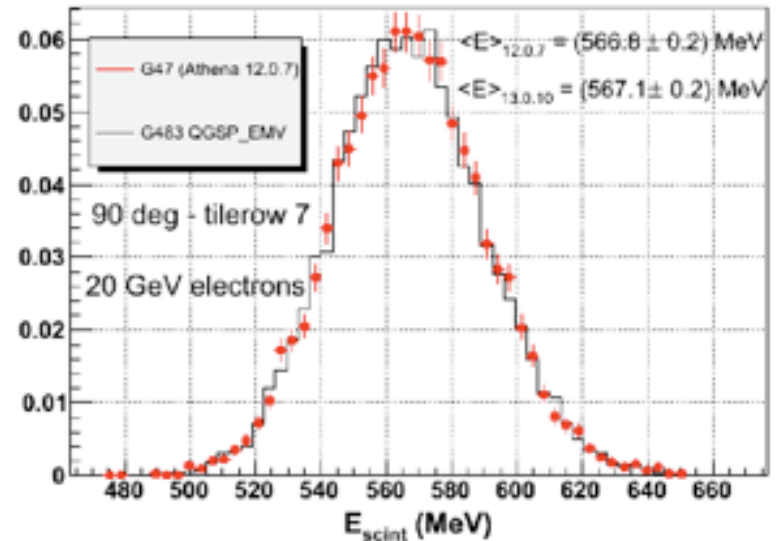
- **Pseudoprojective** and $\theta=\pi/2$ configuration: the beam is impinging “unnaturally” (parallel to the ATLAS beam line) on TileCal; a configuration possible only at TBs.
- The beam is always a square - **20 GeV** electrons – no beam divergency simulated.
- **ATHENA 13.0.10** and **G4.83** using different physics lists:
 - **QGSP_EMV**: it is supposed to be the same as G4.7 concerning electromagnetic showers.
 - **QGSP**: modified multiple scattering.
 - **QGSP_BERT**: model for intra-nuclear nucleon-nucleon scattering (concerning electrons, we expect an energy release very similar to QGSP)
- **ATHENA 12.0.07** and **G4.7**:
 - **QGSP** physics list
- All the results are at the hits level: no electronics noise, no photostatistics, no digitization is applied.
- For all the configurations the setup is TileCal standalone TB.

Given the new multiple scattering, it is expected to be different for **G4.7** and **G4.8**.
We want to estimate this difference.



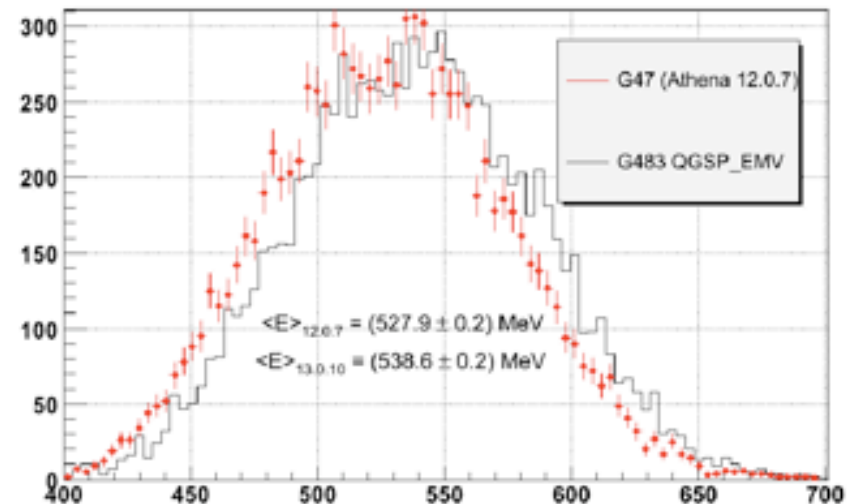
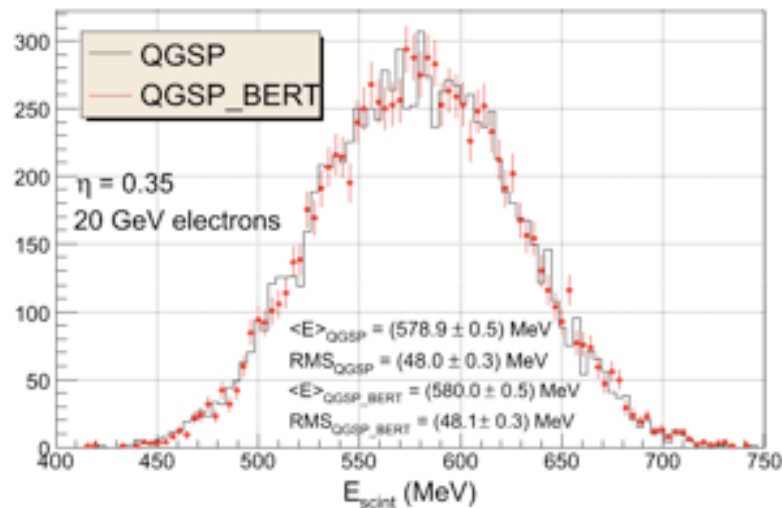
QGSP and **QGSP_BERT** expected to be the same concerning electrons energy release:

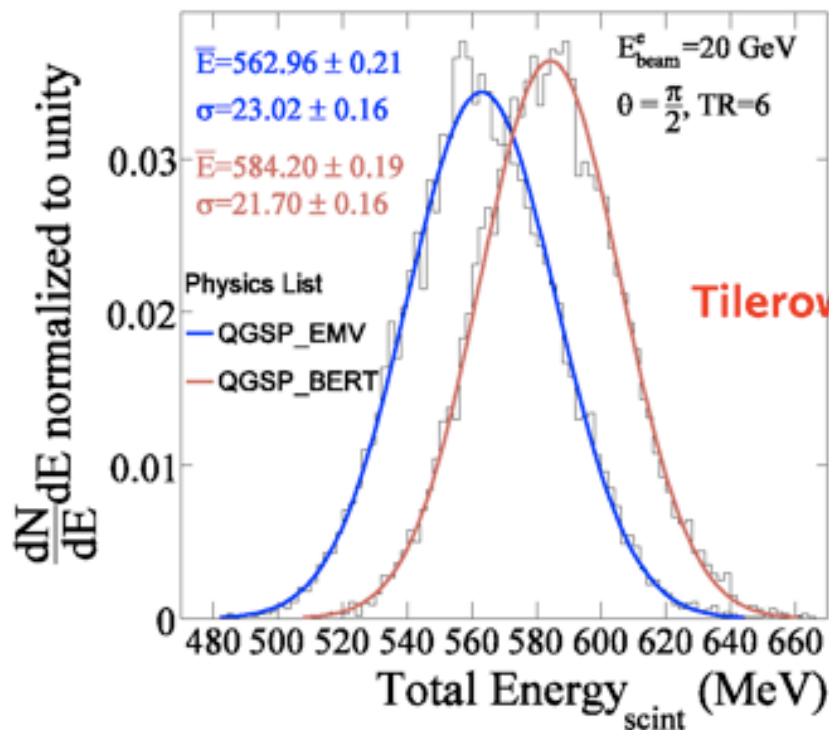
- confirmed for $\theta = \pi/2$ – discrepancies on the mean values at 3 permille.
- confirmed also in pseudoprojective runs



QGSP_EMV:

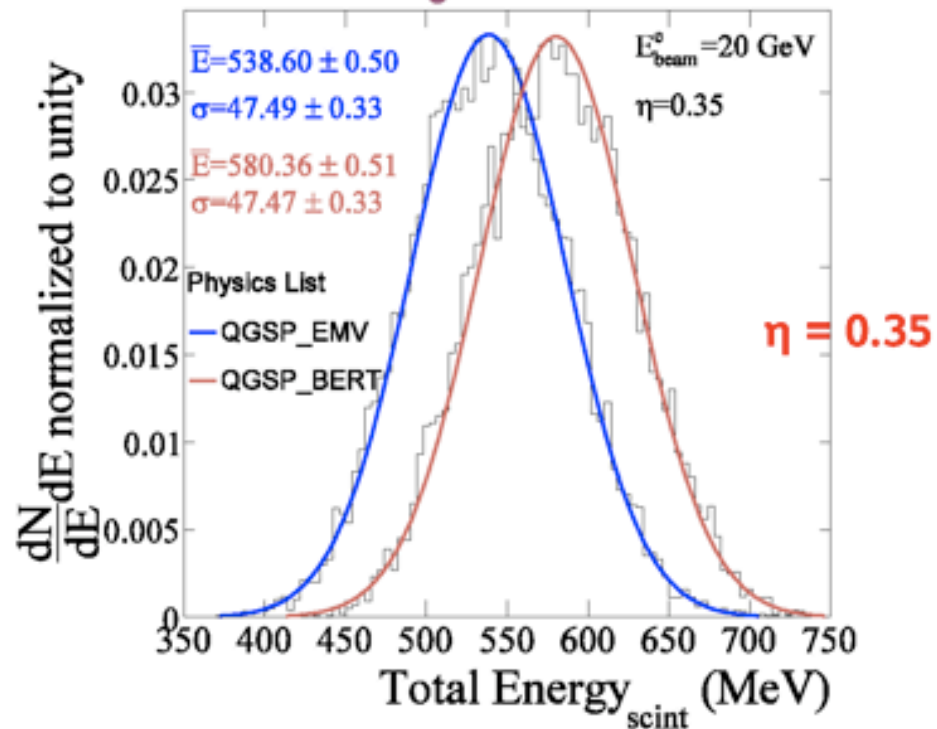
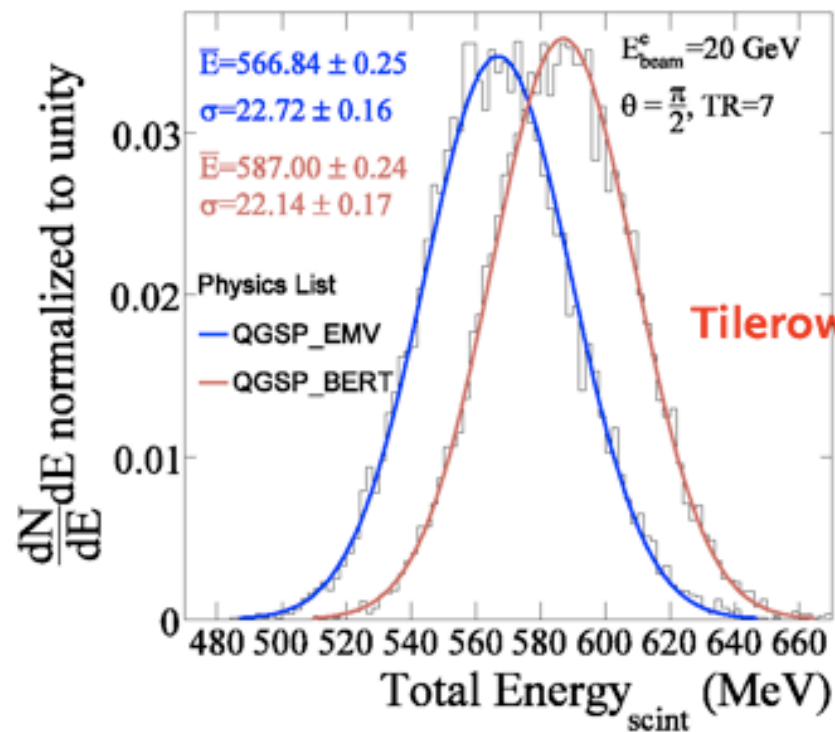
- expected to reproduce G4.7 – confirmed for $\theta = \pi/2$ – the mean values agree within the errors
- is 2% higher with respect to G4.7 for $\eta = 0.35$





Comparison of the energy distributions of QGSP_BERT and QGSP_EMV for two different tilerows

Comparison on the mean value between QGSP and QGSP_EMV shows a different ratio between sampling fractions w.r.t. the 90 deg configuration (left plots)



Summarizing on sampling fraction

Physics list	$\theta = \pi/2$	$\eta = 0.35$
$QGSP_{EMV}$ and G4.7 predict the same mean energy in the scintillators?	yes	no $QGSP_{EMV}$ is higher w.r.t. G4.7 by 2%
$QGSP_{EMV}$ and $QGSP_{BERT}$ predict the same mean energy in the scintillators?	yes	yes
Ratio $\frac{\langle E \rangle_{QGSP_{EMV}}}{\langle E \rangle_{QGSP_{BERT}}}$ where the error is the maximum spread between tilerows :	0.965 ± 0.002	0.928 ± 0.002
The G4.7 sampling fraction is 1/35.9		
Simulating $QGSP_{EMV}$ with the same sampling fraction might result in a 2% excess in energy (projective result).		
$QGSP$ and $QGSP_{BERT}$ sampling fraction is the same within 1% level at 90° and at $\eta = 0.35$. More eta points can shed light to the pseudorapidity dependence.		
Our present results show that $QGSP_{BERT}$ sampling fraction is $1/(34.3 \pm 0.2)$, where the error indicates the spread $90^\circ - \eta = 0.35$.		

Local Hadron Calibration

Sven Menke

- * Use clusters (instead of towers) as input to jet clustering algorithms
- * Clusters are corrected for:
 - * “Hadronic energy losses” (i.e. clusters originating from charged pions) corrected for non-compensation
 - * Energy losses in dead material (between and in front of calorimeters)

Local Hadron Calibration

1st Artemis Annual Meeting

Sven Menke, MPI München

27. September 2007, Chalkidiki, Greece

▶ Local Hadron Calibration

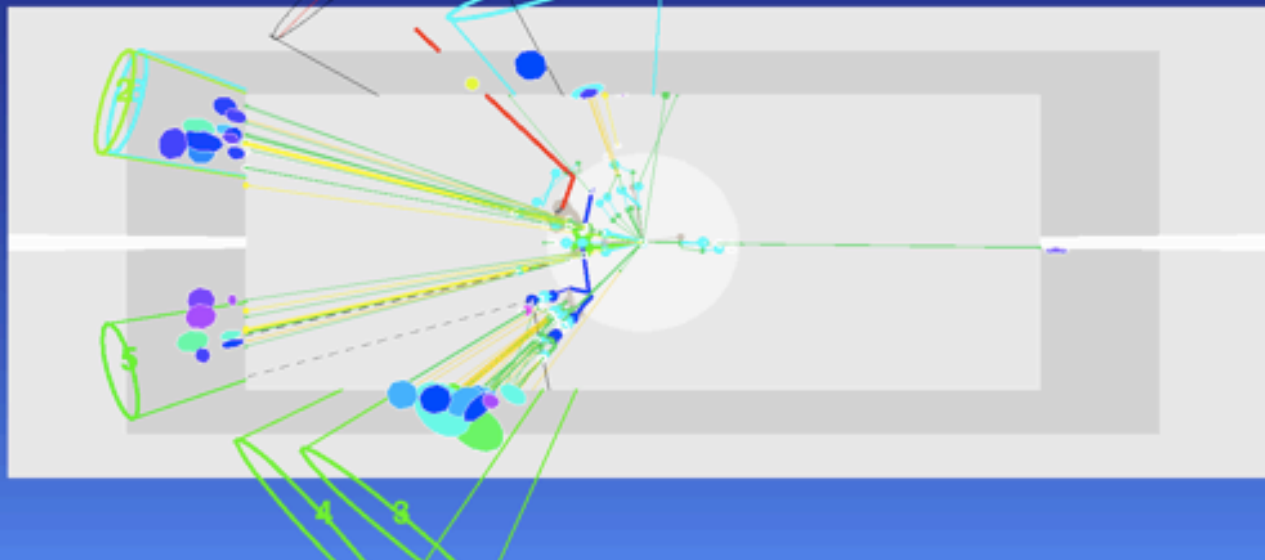
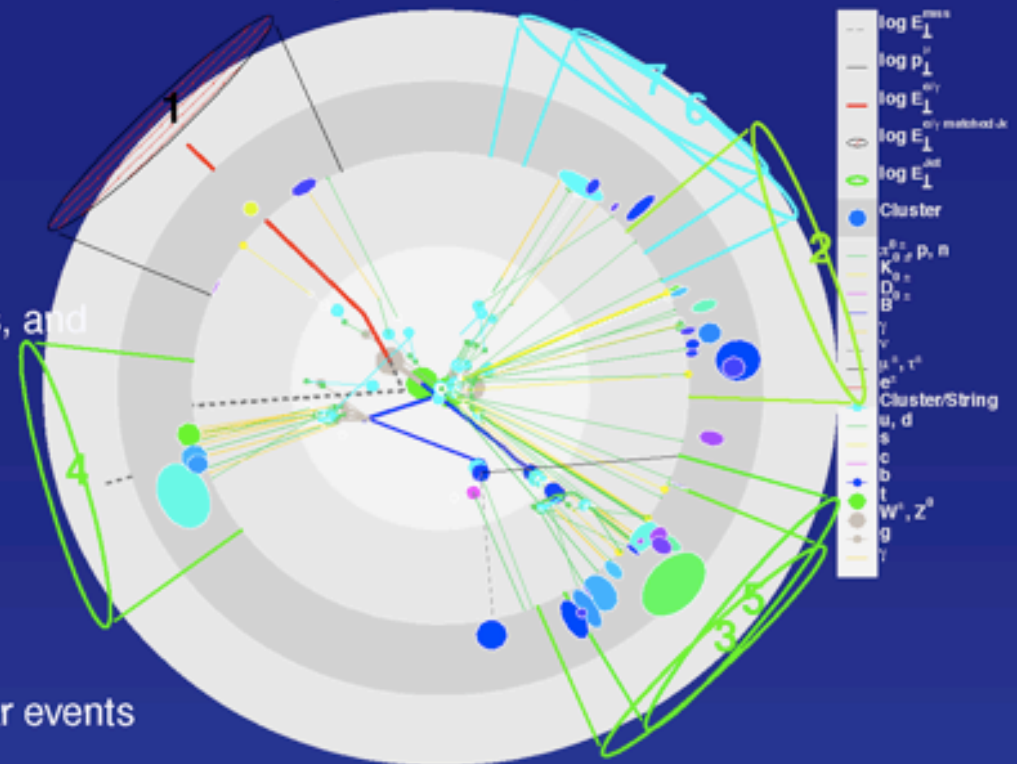
- cluster moments and classification
- energy weights, dead material corrections, and out-of-cluster corrections

▶ Application to jets

- jet level corrections

▶ Plans

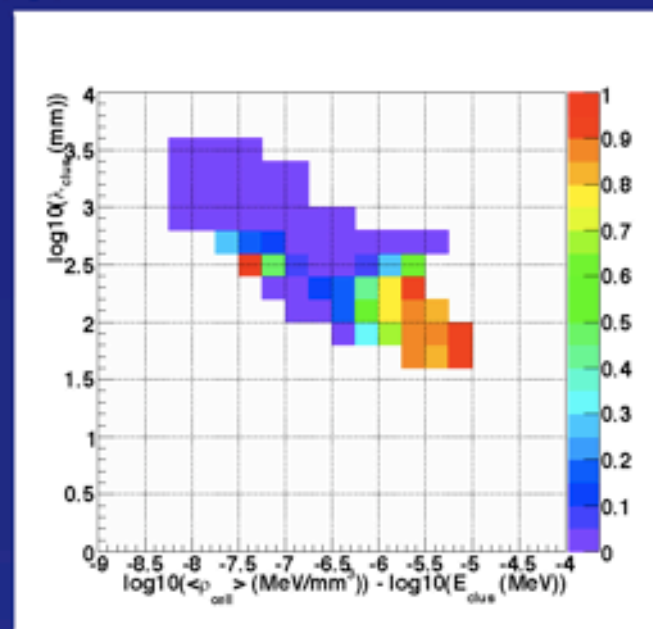
- top-mass measurements in hadronic tt-bar events



Local Hadron Calibration

- ▶ Classify and calibrate topo clusters to hadron-level
- ▶ Classification

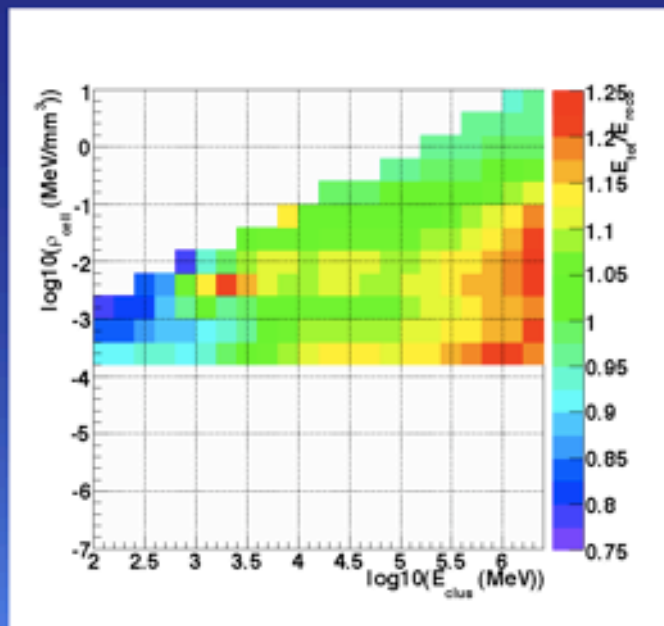
- use shower shape variables (cluster moments) like shower depth and (weighted) energy density of the cell constituents normalized to cluster energy
- em showers are less deep and have higher average energy density than had showers
- derive phase space population in energy-depth-density space for charged and neutral pions
- make a cut on probability to observe a neutral pion with a-priori neutral-to-charged pion ratio of 1 : 2 (example plot shows endcap and $8 \text{ GeV} < E_{\text{clus}} < 16 \text{ GeV}$)

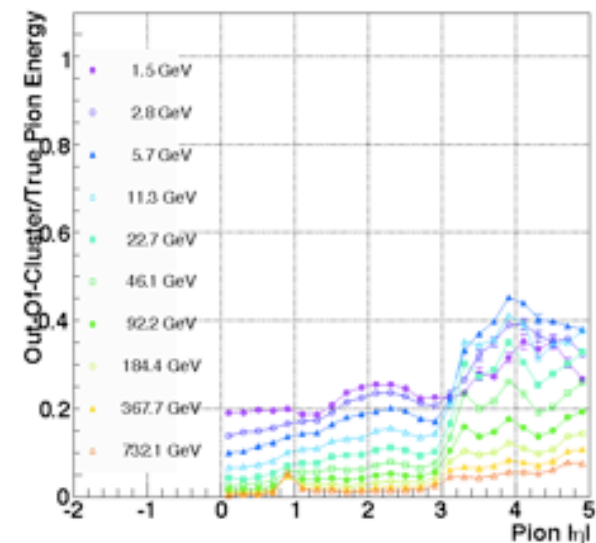
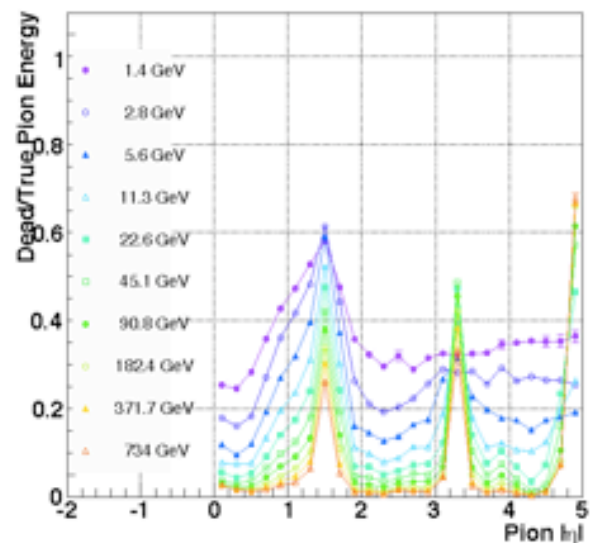
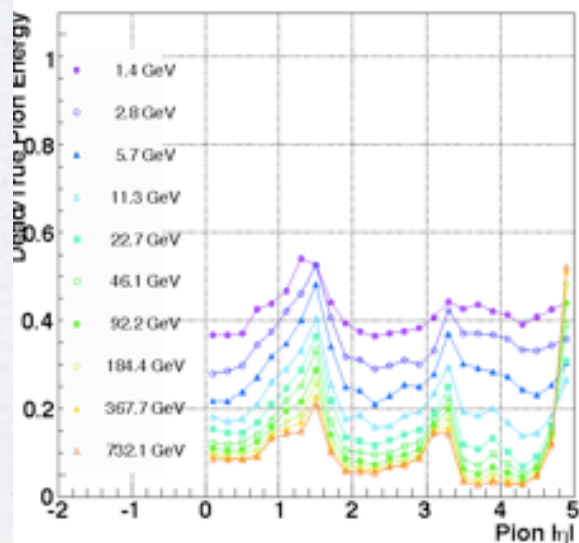


▶ Calibration

- treat only clusters classified as hadronic
 - ▶ except for dead material corrections which are available also for em clusters
- derive cell weights from Geant4 true energy (calibration hits) including invisible energy and absorber deposits and reconstructed cell energy for each η region and layer:
$$w_i = \langle E_{\text{true}} / E_{\text{reco}} \rangle, i = \text{bin}\#(E_{\text{cluster}}, E_{\text{cell}} / V_{\text{cell}})$$
- example weights in main sampling of EM calorimeter for $2.0 < |\eta| < 2.2$

▶ Apply dead material and out-of-cluster corrections





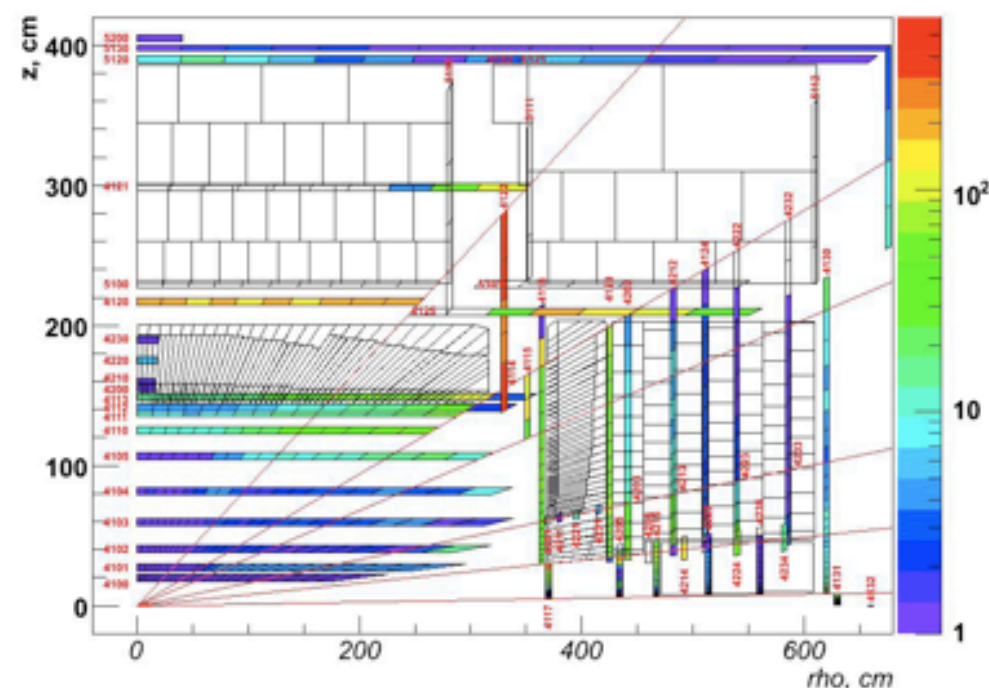
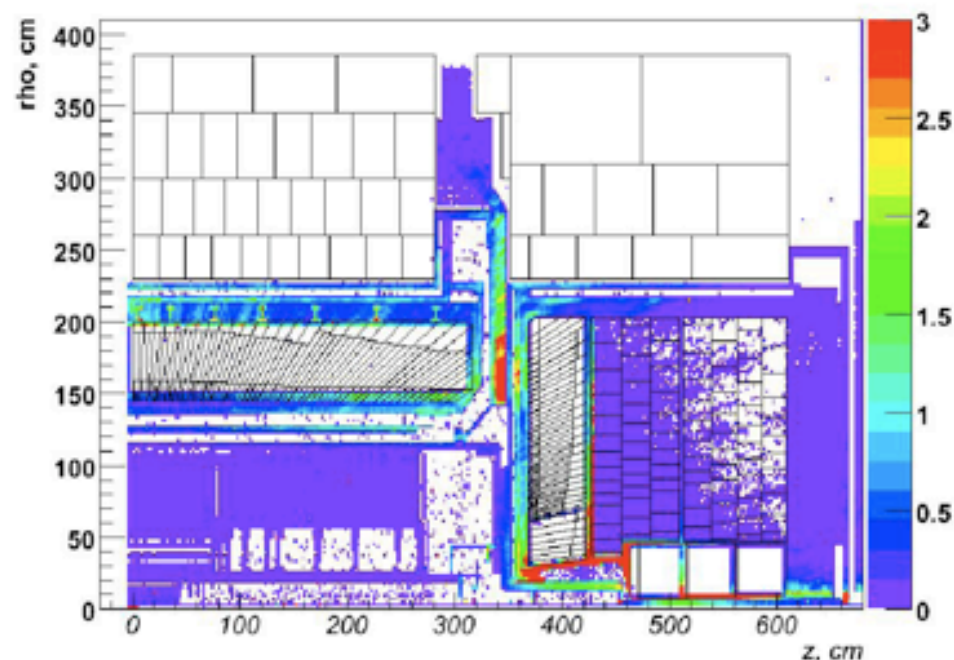
▶ Dead material corrections

- account for deposits in material in front of and between calorimeter systems overlapping in $\eta \times \phi$ with cells from the cluster
- for charged pions (left plot)
- for neutral pions (right plot)

▶ Out-Of-Cluster corrections

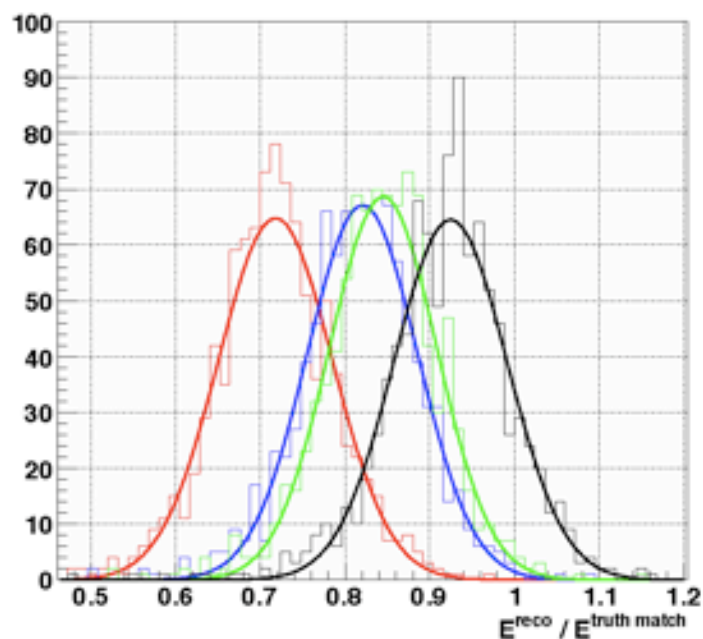
- account for all the rest
- mainly deposits in calorimeter cells left out by the cluster algorithm
- weighted with degree of isolation of the cluster to avoid double-counting

- Average G4Hit's energy deposited in dead material for 100 GeV pions (left)
- Dead Material Hits are saved in 53 separate areas with granularity $\Delta\eta \times \Delta\phi = 0.1 \times 0.1$ (right)
- corrections are derived from cell energies inside topo clusters close to the DM areas
- task is to find correlations of measured energies with expected (predicted) DM deposits



Local Hadron Calibration ► Performance

- Use two leading jets (K_{\perp} with $R = 0.4$) in di-jet MC samples in the region $0.2 < |\eta| < 0.4$
- Energy of the leading jets in this sample and region is about 150 ± 40 GeV
- plot shows the ratio of total energy of the reconstructed jet over the energy of a matched truth jet (also K_{\perp} with $R = 0.4$) with $\Delta R < 0.05$ for EM-scale (red); weighted (blue); weighted+OOC (green); weighted+OOC+DM (black)



	EM	W	W+OOC	W+OOC+DM
mean (%)	71.8	82.0	84.5	92.5
σ (%)	6.7	6.5	6.3	6.7
σ/mean (%)	9.4	7.9	7.5	7.2

- mean and relative resolution improve in every step
- final deviation from truth jet energy is only 7.5 % consistent with expected out-of-jet corrections ($\sim 3\%$ cluster inefficiency; $\sim 3\%$ misclassification; $\sim 2\%$ magnetic bending)

Plans

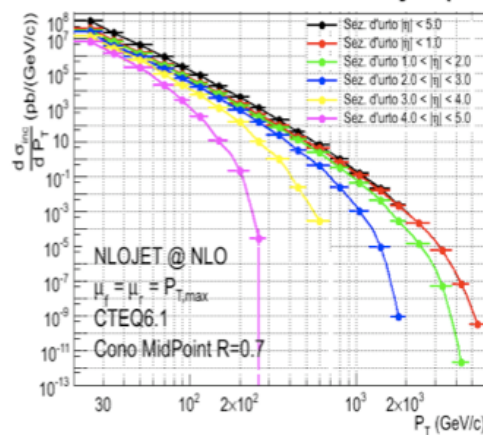
- ▶ Artemis PhD student (P. Giovannini) starts end of October
 - development of jet-level corrections on top of local hadron calibration
 - ▶ the final 7.5% for jet energy response
 - application of in-situ weighting to parton level in tt-bar events
 - ▶ the go from hadron to parton level
 - measurement of the top-mass in the all hadronic channel
 - ▶ this channel relies most on jet performance
- ▶ Maintenance and further improvements of local hadron calibration within the MPI/HEC group
 - ▶ especially the 3% due to misclassification need to be addressed
- ▶ Commissioning and top-mass measurement in the semileptonic top-pair channel within the MPI/HEC group
 - ▶ 2 more ongoing PhD studies

Towards first measurements: inclusive jet cross section

Paolo Francavilla

- * First attempt to study systematic uncertainties in inclusive jet cross section measurements:
 - * Theoretical uncertainties: uncertainties on LO vs NLO calculations, renormalization and factorization scales, uncertainties on PDFs
 - * Experimental uncertainties: effect of jet energy scale and of jet resolution
- * Studies performed on parton jets only (generator level)

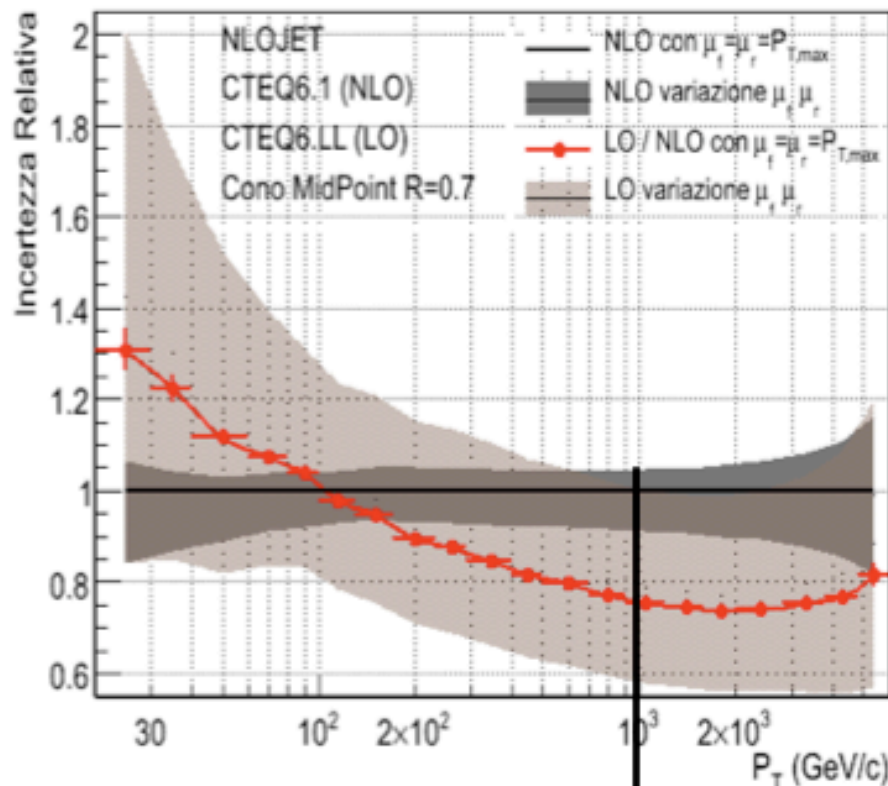
Sezione d'urto inclusiva dei jet (NLO)



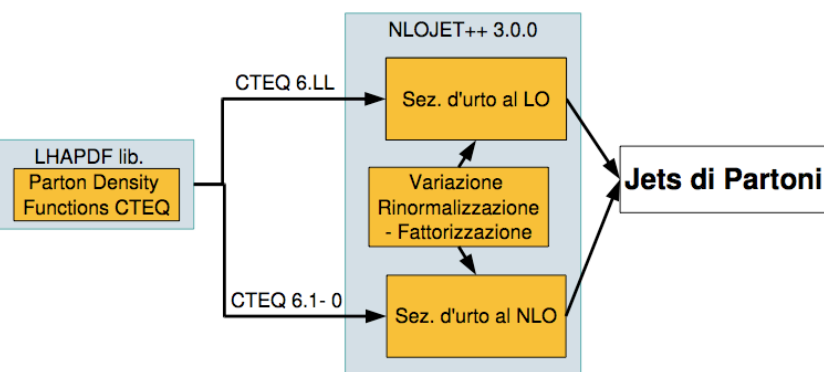
- * Studied difference in predicted inclusive jet cross-section between LO and NLO calculations

- * Renormalization (μ_r) and factorization (μ_f) scales have been varied and effect on cross section has been studied

Ordini successivi - Incertezza sezione d'urto $|\eta| < 5.0$



Incertezze:
 ~30% @LO (1 TeV/c)
 ~7% @NLO (1 TeV/c)

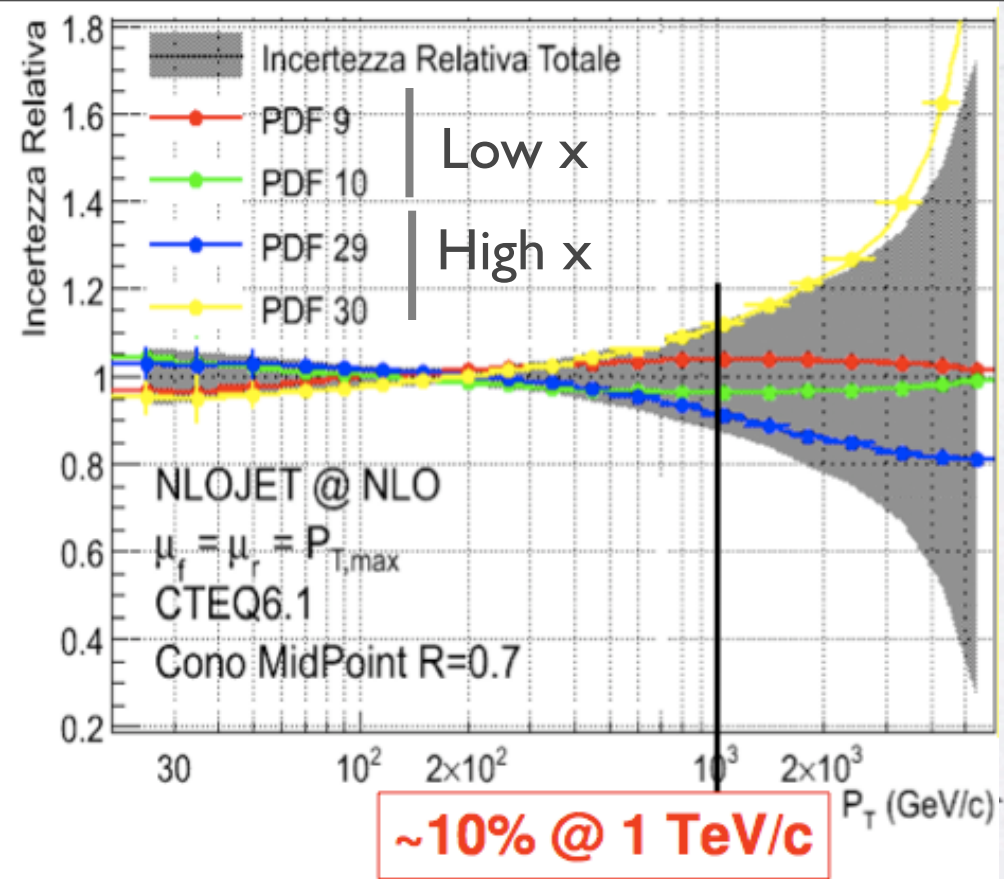


μ_r	μ_f
$0.5 P_t^{\text{jet Max}}$	$0.5 P_t^{\text{jet Max}}$
$1.0 P_t^{\text{jet Max}}$	$1.0 P_t^{\text{jet Max}}$
$2.0 P_t^{\text{jet Max}}$	$2.0 P_t^{\text{jet Max}}$

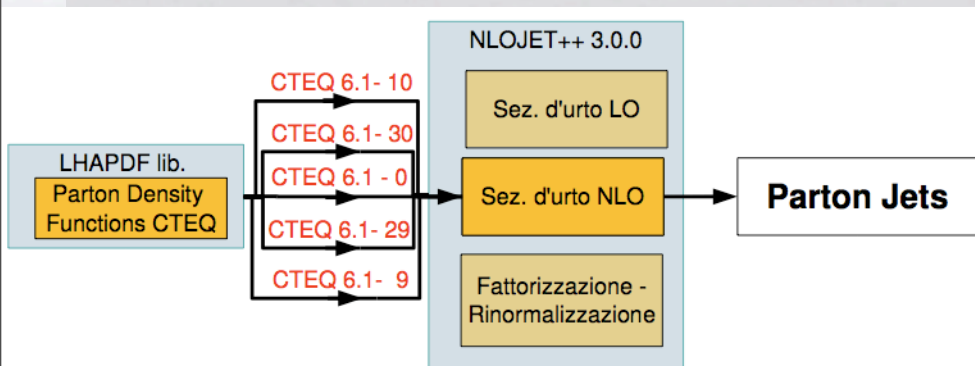
* Uncertainties in PDFs influence cross section measurement

* Total uncertainty dominated by gluon PDF contribution

* Effects of uncertainty at low x (9-10) and high x (29-30) have been studied



* At high transverse momentum uncertainties on high x gluon PDFs largely dominate



* Effect of jet energy scale:

* Effect of jet energy resolution:

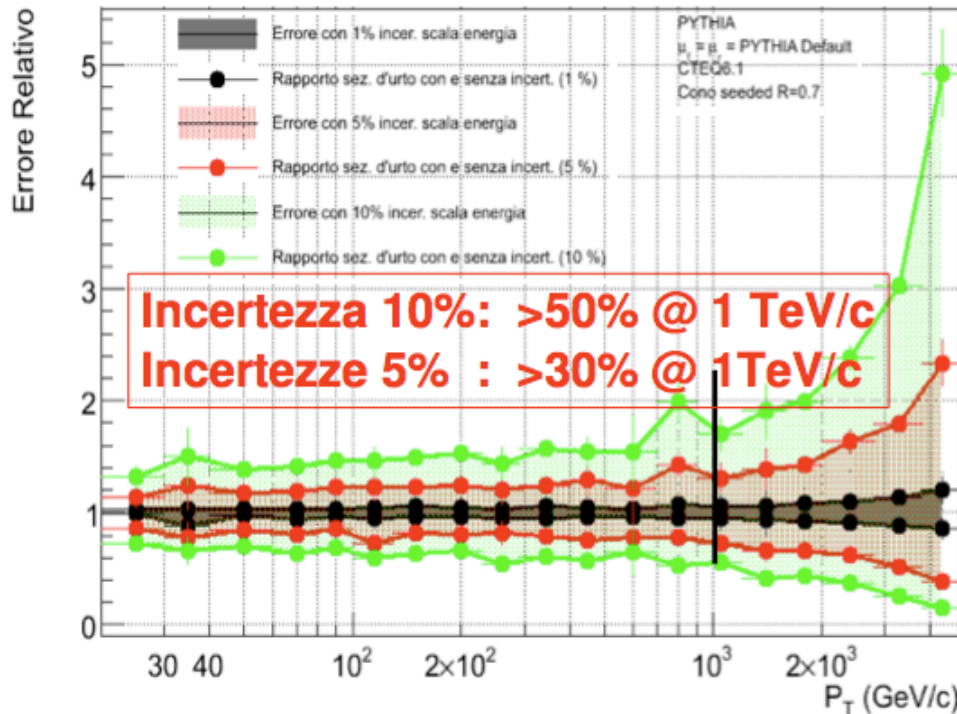
◇ * $P_T' = (1+x)P_T$

* $\sigma(E)/E = a(1+x)/\sqrt{E} \oplus b(1+x)/E \oplus c(1+x)$ ◇

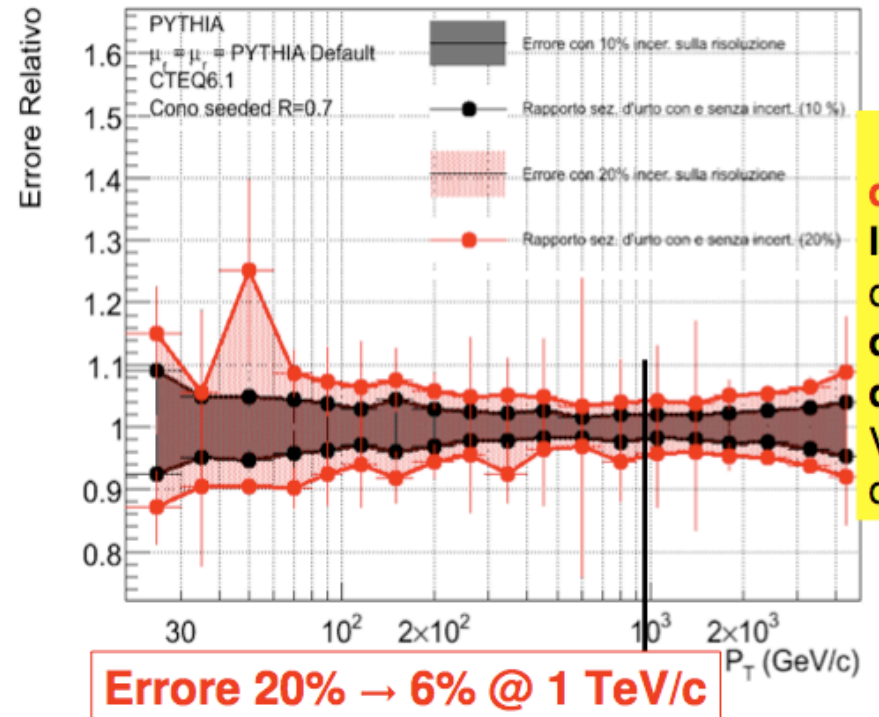
* $x = \pm 1\%, \pm 5\%, \pm 10\%$

* $x = \pm 10\%, \pm 20\%$

Errore sez. d'urto: Effetto incert. scala di energia dei jet



Errore sez. d'urto: Effetto dell'incertezza sulla risoluzione



source	$P_T = 1 \text{ TeV}/c$	$P_T = 200 \text{ GeV}/c$
Jet Energy scale 10% (5%)	57% (29%)	43% (21%)
PDF	13%	2%
Renorm. and Fact. scales (NLO)	7%	6%
Jet Resolution 20% (10%)	4% (2%)	6% (3%)
Stat. (100 pb^{-1})	1.2%	2%

Calibration method (HI) verified on CTB data, O(5%) JES error seems reasonable.

See V. Giangiobbe talk



* Many thanks to Sven, Zenon and Paolo